Songklanakarin J. Sci. Technol.
47 (2), 151–159, Mar. – Apr. 2025

http://www.sjst.psu.ac.th

Original Article

Performance of CMIP6 climate models in assessing the ground observed climatic variables: A comparative study using statistical approach

Gopeshwar Sahu and Vikas Kumar Vidyarthi*

Department of Civil Engineering, National Institute of Technology Raipur, Raipur, Chhattisgarh, 492010 India

Received: 25 May 2024; Revised: 22 February 2025; Accepted: 8 April 2025

Abstract

Climate models are essential for understanding and predicting precipitation and temperature patterns, which are fundamental to facilitate effective water resource management and the implementation of sustainable practices in a variety of sectors such as urban planning, agriculture, and preserving biodiversity. The purpose of this study is to assess the comparative performance of the outputs of the twenty global climate models (GCMs) from Coupled Model Intercomparison Project Phase 6 (CMIP6) to accurately simulate patterns of precipitation (PPT), maximum temperature (TMAX), and minimum temperature (TMIN) across the Mahanadi River basin in Chhattisgarh, India, between 1985 and 2014. The evaluation of CMIP6 models against observational data involved the utilization of several statistical metrics, including coefficient of determination (R^2), Nash-Sutcliffe efficiency (NSE), Kling-Gupta efficiency (KGE), Percent bias (PBIAS), and the Taylor diagram. Using these statistics, it has been found that the CMIP6 model MIROC-ES2L outperforms the others for PPT and TMIN, whereas the model IPSL-CM6A-LR is superior to the others for TMAX in the study region. While working with the CMIP6 models researchers and hydrologists can use the outcome of this study for useful insights to predict and adapt to changing climatic trends, which may help them in making well-informed decisions for sustainable and adaptable water resource management within the study region.

Keywords: global climate model, CMIP6, statistical analysis, Mahanadi River basin, Taylor diagram

1. Introduction

The Global Climate Models (GCMs) incorporate physical equations and data from various sources to simulate the behavior of the climate system over long periods of time. These models are used to understand and study climate patterns, predict future climate scenarios, and assess the potential impacts of various factors such as greenhouse gas emissions on the Earth's climate (Chokkavarapu & Mandla, 2019). They took into account factors such as solar radiation atmospheric composition, land surface characteristics, and other variables to generate projections of climate patterns at global, regional, and local scales (Giorgi, 2019). Coupled Model Intercomparison Project Phase 6 (CMIP6) is a worldwide climate model intercomparison projection that provides an insightful opportunity to investigate past and future variations in mean and extreme climates at the regional and global levels (Mathbout, Martin-Vide, & Bustins, 2023). CMIP6 projections can be employed to analyze future changes in precipitation, temperature, and other climatic variables which are at finer resolutions, and these variables have an influence on runoff and other hydrological variables on a local scale (Ali *et al*., 2023). Out of all the climatic variables, precipitation and temperature are major inputs in the context of the simulation of runoff and predicting floods or droughts (Brunner, Slater, Tallaksen, & Clark, 2021). The floodplains of rivers are frequently altered by changing population and land use trends, as well as climate change (Hazarika, Das, & Borah, 2015). These variables are accountable for the uncertainty in hydrological performance assessment (Dibaba, Demissie, & Miegel, 2020). Thus, exact measurements of precipitation and temperature will be difficult due to their irregularities and biased statistics at the regional and local levels. In this regard, the use of CMIP6 models is vital

*Corresponding author
Email address: vkvidyarthi.ce@nitrr.ac.in;
vikas.civil@gmail.com

because it provides an advanced framework for understanding and projecting these complex precipitation and temperature dynamics, providing valuable insights for sustainable water resource management and agricultural planning in the context of India's changing climatic conditions (Kushwaha, Pandey, Kumar, Sardana, & Yadav, 2024). Before using GCM outputs, it is recommended that relative bias or uncertainty in these data must be removed by comparing them to observational data (Ngai, Tangang, & Juneng, 2017). The ability of GCMs to simulate historical climate is dependent on the modeling trend, encompassing the precision of the model network and the scientific recognition of specific physical processes such as radiative forcing and land surface interactions (Chokkavarapu & Mandla, 2019).

Appropriate GCM selection is critical for removing uncertainty and improving the reliability of climate variables such as precipitation and temperature (Raju & Kumar, 2020). Considering this, there is currently no prevailing technique or established standards for GCM selection. However, it is commonly assumed that selected GCMs will correctly mimic historical climate properties such as mean, variance, and spatial variability (Hamed, Nashwan, & Shahid, 2022). Several researchers examined the performance of GCMs in mimicking climate variables using statistical indices such as relative bias, Taylor diagram, correlation coefficient, relative error, and root mean square error (Gleckler, Taylor, & Doutriaux, 2008; Lambert & Boer, 2001). However, the comparison is limited to a few GCMs only, and also a comprehensive comparison is still missing for implementing them at the local scale.

CMIP6 projects potential shifts in precipitation patterns, temperature, and extreme events by offering detailed climate model simulations and projections, assisting in developing adaptive approaches for safeguarding water resources effectively in the context of climate change (Haider *et al*., 2023). However, before employing forecasts, it is important to assess model reliability by comparing model outputs to observational data. This examination reveals biases, ensuring accurate projections that are critical for informed decisions as well as effective strategies to reduce the effects of climate change. Considering all of these factors the purpose of this study is the comparative analysis of CMIP6 models in mimicking climatological variables over the Mahanadi River basin in Chhattisgarh State, India with the following specific objectives: a) to compare the performance of CMIP6 climate models for precipitation (PPT) using various statistical measures; b) to compare the performance of CMIP6 climate models for maximum and minimum temperatures (TMAX and TMIN) using various statistical measures; c) to rank each CMIP6 models for PPT, TMAX, and TMIN over the study area. The Mahanadi River basin is significantly impacted by the intrinsic threats of climate change, such as alterations to precipitation patterns and surface hydrology, which cause floods, and extended drought.

The paper begins with an overview of the tools and techniques used in this study. Following a description of the study area and the data used, the paper goes on to present the results and discussions on different statistics calculated for the various climatic variables over the years. Finally, the paper ends with the conclusions drawn from the study.

2. Tools and Techniques

The study examines the performance of twenty different CMIP6 GCMs by assessing their ability to recreate historical climate data from 1985 to 2014. For this purpose, various statistical indices such as the Coefficient of Determination (R^2), Nash-Sutcliffe efficiency (NSE, Nash & Sutcliffe, 1970), Kling-Gupta efficiency (KGE, Gupta, Kling, Yilmaz, & Martinez, 2009), Percent bias (PBIAS), and the Taylor diagram (Taylor, 2001) are used to measure similarities and compare GCMs to the observed pattern of climatic data. R^2 is a statistical measure of similarity between two datasets that ranges from 0 to 1. A greater value indicates more similarity. NSE is frequently used in hydrological and environmental modeling to evaluate the precision of a model by comparing with observed data (Xie *et al*., 2019). It has a range of $-\infty$ to 1, where a value closer to 1 denotes a higher level of model efficacy. KGE is mostly used in hydrological modeling and water resource management to assess models' ability to replicate observed datasets (Ahmed, *et al*., 2019). It was built on multi-criteria evaluation statistics, which include three components: correlation, biases, and variability. KGE values vary from $-\infty$ to 1, with values closer to 1 indicating better performance of the model. PBIAS is the percentage difference between the simulated model and the observed dataset. Positive values in the PBIAS reveal overestimation bias, negative values imply underestimation bias and a PBIAS value of 0 shows no bias. For a detailed description of each statistical measure and its associated formula, interested readers may refer to the following literature: Gupta *et al*. (2009), Legates and McCabe (1999), Nash and Sutcliffe (1970). Each GCM is ranked based on the values of the scores from various statistical indices. Then, the sum of the scores from each index is used to establish the overall ranking.

Taylor diagrams (Taylor, 2001) are mathematical visualizations used to compare the accuracy of multiple statistical models by graphically representing the correlation, root mean square error (RMSE), and standard deviation ratio between IMD observed and CMIP6 simulated climatic variables datasets.

3. Study Area and Data Used

The Mahanadi River, India's eighth-largest basin and a major peninsular river, flows from Sihawa in Chhattisgarh's Dhamtari district to the Bay of Bengal. The Mahanadi River basin is one of India's most vulnerable regions to climate change. The river's overall length is around 851 kilometers and passes from many states, however, the study area is Mahanadi in Chhattisgarh state only as shown in Figure 1. Figure 1 also shows the variation of annual rainfall over the basin. The basin is primarily drained by the Seonath, Arpa, Pairi, Sukha, and Hasdeo Rivers as major tributaries.

The climate of this region is primarily subtropical, and the temperature varies from 4℃ to 12℃ during the winter, and from 39℃ to 40℃ during the summer. The maximum rainfall occurred between July and September, with values ranging from 800 to 1,200 mm. The basin is dominated by forested hills, fertile plains, and plenty of vegetation. The observed daily temperature and precipitation for 83 grids with

a resolution of 0.25°x 0.25° were obtained from the Indian Meteorological Department (IMD), Pune from 1985 to 2021. CMIP6 precipitation and temperature data are derived from NASA's Earth Exchange Global Daily Downscaled Projections-Coupled Model Intercomparison Project Phase 6 (NEX-GDDP-CMIP6), which has been statistically bias-corrected (using Bias-Correction Spatial Disaggregation method) and has a high spatial resolution of 0.25°x 0.25° in daily time steps. The downscaled data for these GCMs were obtained from the NASA portal (https://www.nccs.nasa.gov/services/data-collections/land-based-products/nex-gddp-cmip6, retrieved on 10-Oct-2023) and the twenty CMIP6 models developed by different agencies across the globe whose performance in mimicking various climatic variables assessed in this study are described in Table 1. These GCMs are selected based on availability of data for Mahanadi River basin and are popularly utilized by researchers (Zamani, Monfared, Moghaddam, & Hamidianpour, 2020; Hemanandhini, 2023).

4. Results and Discussion

The performances of all the twenty CMIP6 models in mimicking PPT, TMAX, and TMIN with corresponding IMD observations of these variables have been assessed using various statistical measures and the Taylor diagram. Table 2 shows the quantitative analysis of various statistical measures for monthly mean PPT across various CMIP6 models in comparison to IMD observed PPT data. The rankings assigned to each measure, and then the sum of these rankings, highlight the overall performance of a specific model. From Table 2, it can be observed that the CMIP6 model MIROC-ES2L

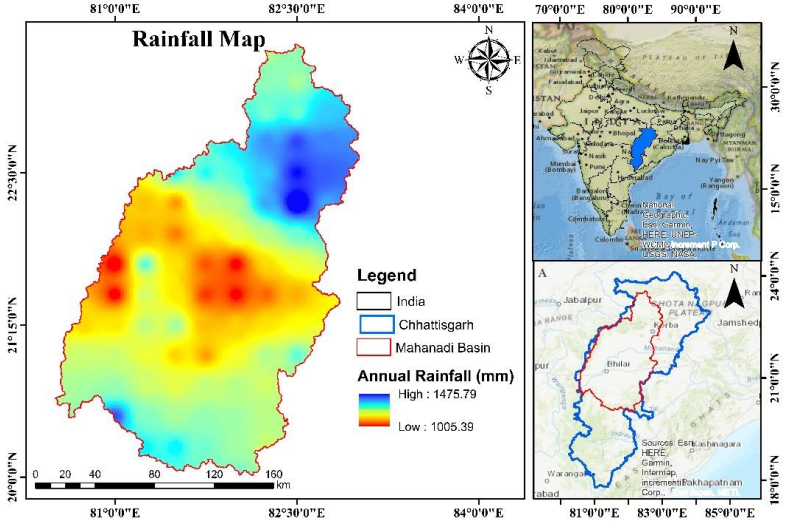

Figure 1. Mahanadi River basin, Chhattisgarh, India and variation of annual rainfall over the basin

Table 1. CMIP6 Models used in this study

S. NO.	CMIP6 Model	Institute/Agency
1	ACCESS-CM2	Australian Community Climate and Earth-System Simulator
2	ACCESS-ESM1-5	Australian Community Climate and Earth-System Simulator
3	BCC-CSM2-MR	Beijing Climate Center and China Metrological Administration
4	CAN ESM5	Canadian Centre for Climate Modelling and Analysis, Canada
5	CMCC-ESM2	Fondazione Centro Euro-Mediterraneo sui Cambiamenti Climatici, Italy
6	CNRM-CM6-1	National Centre for Meteorological Research, France
7	CNRM-ESM2-1	National Centre for Meteorological Research, France
8	EC-Earth3	EC-Earth consortium, Europe
9	EC-Earth3-Veg-LR	EC-Earth consortium, Europe
10	FGOALS-g3	Chinese Academy of Sciences, China
11	GFDL-ESM4	Geophysical Fluid Dynamics Laboratory, USA
12	GISS-E2-1-G	Goddard Institute for Space Studies, USA
13	INM-CM5-0	Institute for Numerical Mathematics, Russia
14	IPSL-CM6A-LR	Institute Pierre Simon Laplace, France
15	MIROC-ES2L	Atmosphere and Ocean Research Institute (The University of Tokyo), National Institute for Environmental Studies, and Japan Agency for Marine-Earth Science and Technology, Japan
16	MPI-ESM1-2-LR	Max Planck Institute for Meteorology, Germany
17	MPI-ESMI-2-HR	Max Planck Institute for Meteorology, Germany
18	MRI-ESM2	Meteorological Research Institute, Japan
19	NOR ESM2-MM	Norwegian Climate Centre, Norway
20	NorESM2-LM	Norwegian Climate Centre, Norway

outperformed the other models with a high R^2 (0.81), a high NSE (0.80), an excellent KGE (0.90), and a satisfactory PBIAS (-2.93), making it the most suitable choice for mimicking PPT in the study region. The graphical representations in terms of bar chart and radar diagram are presented in Figure 2(a) and Figure 2(b), respectively, which provide a clear visual understanding that aids in the identification of the most effective model by comparing the CMIP6 simulated output with IMD observed data to mimic PPT. The graphical representation supports the quantitative analysis by adding a layer of insight, making it simpler to detect the performance of the models. The bar charts highlight the relative performance across different metrics such as R^2, NSE, KGE, and PBIAS, while the radar charts provide a holistic view by showcasing the models across multiple criteria simultaneously. The performance of each metric is shown on a radar chart as the radial distance from the center and the best model is shown as a solid line with a shaded region. It can be observed from Figure 2(a) and Figure 2(b) that the MIROC-ES2L CMIP6 model outperforms the other

Table 2. Performance evaluation measures of CMIP6 models with IMD observed data for PPT

CMIP6 MODEL	R^2	NSE	PBIAS	KGE
ACCESS-CM2	0.61	0.41	4.48	0.69
EC-Earth3	0.65	0.57	-1.29	0.78
GFDL-ESM4	0.60	0.54	-9.61	0.75
INM-CM5-0	0.58	0.45	-4.95	0.73
CAN ESM5	0.56	0.45	-5.94	0.73
CMCC-ESM2	0.61	0.54	-1.45	0.77
MPI-ESMI-2-HR	0.72	0.67	-2.67	0.84
MRI-ESM2	0.59	0.53	-10.59	0.75
NOR ESM2-MM	0.65	0.56	1.02	0.78
EC-Earth3-Veg-LR	0.66	0.60	-3.74	0.80
FGOALS-g3	0.68	0.65	-4.81	0.82
ACCESS-ESM1-5	0.57	0.43	-7.01	0.72
GISS-E2-1-G	0.61	0.53	-5.47	0.77
IPSL-CM6A-LR	0.69	0.66	-12.05	0.79
MIROC-ES2L	0.81	0.80	-2.93	0.90
MPI-ESM1-2-LR	0.70	0.67	-3.98	0.83
NorESM2-LM	0.70	0.61	0.62	0.79
BCC-CSM2-MR	0.74	0.72	-2.69	0.86
CNRM-CM6-1	0.63	0.56	-4.35	0.78
CNRM-ESM2-1	0.67	0.61	-3.73	0.80

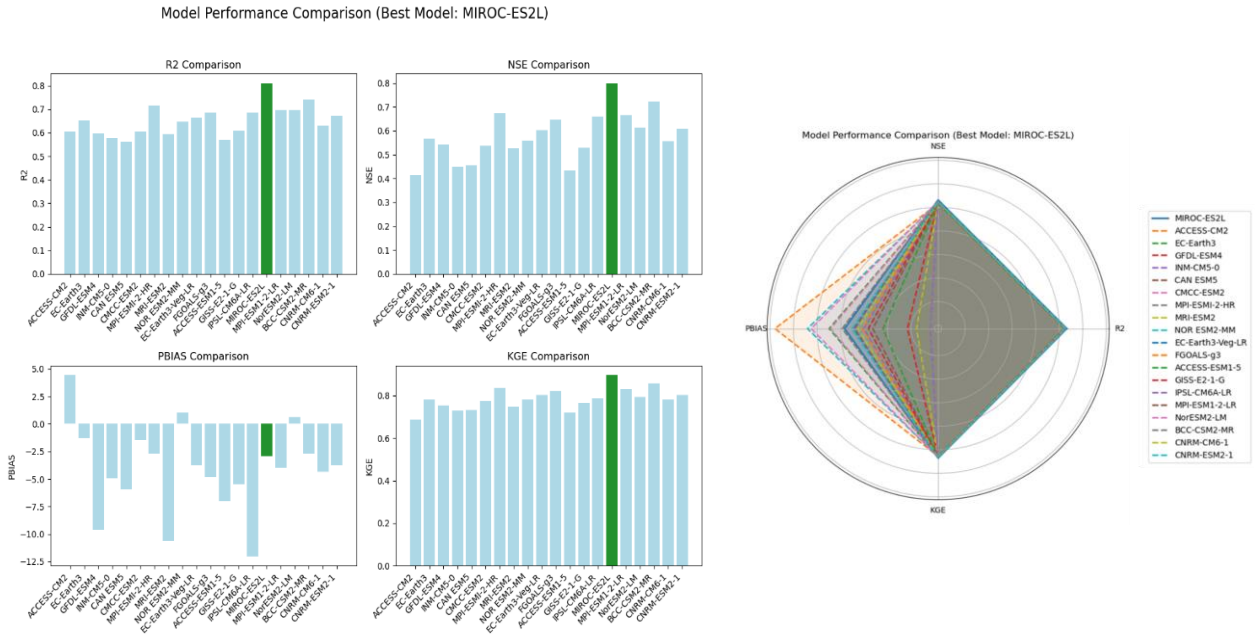

(a) Bar Chart (b) Radar Chart

Figure 2. Performance of various CMIP6 models to mimic PPT over the study region in 1985-2014

models assessed in this study. From both numerical analysis and graphical visualization, it is clear that MIROC-ES2L is the most efficient and reliable model to mimic the PPT.

Similarly, this analysis has been performed for TMAX and TMIN, since these variables are crucial for assessing climate patterns. Table 3(a) shows the different statistics measures of monthly mean data for TMAX across various CMIP6 models in comparison to IMD observation data. From Table 3, it is observed that IPSL-CM6A-LR surpasses the other models for mimicking TMAX with a high R^2 (0.87), a high NSE (0.86), an excellent KGE (0.93), and a good PBIAS (0.49), making it the most efficient preference for TMAX based on these metrics. The graphical representation supports this conclusion that IPSL-CM6A-LR CMIP6 model performs better than the other models in mimicking TMAX, as illustrated in Figure 3. Table 3(b) displays the monthly mean data statistics metrics for TMIN across various CMIP6 models in comparison to IMD observation data. It is noteworthy that MIROC-ES2L performs better than the other models to mimic TMIN because it has a higher R^2 (0.95), a higher NSE (0.92), an excellent KGE (0.91), and a satisfactory PBIAS (4.75), making it the best choice for TMIN based on these metrics. This result is also supported by Figure 4.

Figure 5 depicts the Taylor Diagram, which is based on correlation, standard deviation, and the RMS error matrix. This metric is assessed by comparing each averaged CMIP6 model for the basin to averaged observational datasets collected over a period of 30 years. It is clear that the RMSE is less for the MIROC-ES2L model for PPT. Also, the correlation shown by the inclined line is stronger for the MIROC-ES2L model, and the standard deviation which is

Table 3. Performance evaluation measures of CMIP6 models with IMD observed data for TMAX and TMIN

(a) TMAX

CMIP6 MODEL	R^2	NSE	PBIAS	KGE
ACCESS-CM2	0.83	0.82	-0.69	0.91
EC-Earth3	0.82	0.80	-0.13	0.90
GFDL-ESM4	0.74	0.71	0.01	0.86
INM-CM5-0	0.77	0.74	0.15	0.87
CAN ESM5	0.78	0.76	0.14	0.88
CMCC-ESM2	0.71	0.68	-0.13	0.84
MPI-ESMI-2-HR	0.86	0.85	-0.48	0.93
MRI-ESM2	0.85	0.84	-0.52	0.92
NOR ESM2-MM	0.73	0.70	-0.55	0.85
EC-Earth3-Veg-LR	0.83	0.81	-0.47	0.90
FGOALS-g3	0.86	0.86	-0.06	0.93
ACCESS-ESM1-5	0.84	0.83	-0.23	0.91
GISS-E2-1-G	0.84	0.84	-0.52	0.92
IPSL-CM6A-LR	0.87	0.86	0.49	0.93
MIROC-ES2L	0.85	0.84	-1.04	0.92
MPI-ESM1-2-LR	0.84	0.83	-0.44	0.92
NorESM2-LM	0.85	0.84	-0.37	0.92
BCC-CSM2-MR	0.87	0.85	-0.45	0.92
CNRM-CM6-1	0.84	0.83	-0.26	0.91
CNRM-ESM2-1	0.84	0.82	-0.37	0.91

(b) TMIN

CMIP6 MODEL	R^2	NSE	PBIAS	KGE
ACCESS-CM2	0.91	0.88	5.23	0.93
EC-Earth3	0.92	0.88	6.02	0.91
GFDL-ESM4	0.86	0.82	5.50	0.90
INM-CM5-0	0.87	0.83	5.90	0.90
CAN ESM5	0.87	0.82	5.79	0.90
CMCC-ESM2	0.85	0.82	4.50	0.89
MPI-ESMI-2-HR	0.90	0.85	5.55	0.91
MRI-ESM2	0.93	0.89	5.74	0.90
NOR ESM2-MM	0.84	0.80	4.90	0.90
EC-Earth3-Veg-LR	0.93	0.88	5.87	0.91
FGOALS-g3	0.92	0.87	5.82	0.90
ACCESS-ESM1-5	0.93	0.88	6.03	0.92
GISS-E2-1-G	0.91	0.89	4.09	0.92
IPSL-CM6A-LR	0.92	0.87	6.39	0.91
MIROC-ES2L	0.95	0.92	4.75	0.91
MPI-ESM1-2-LR	0.90	0.86	5.56	0.91
NorESM2-LM	0.91	0.87	5.39	0.92
BCC-CSM2-MR	0.93	0.88	5.52	0.90
CNRM-CM6-1	0.92	0.89	5.09	0.91
CNRM-ESM2-1	0.91	0.88	5.01	0.92

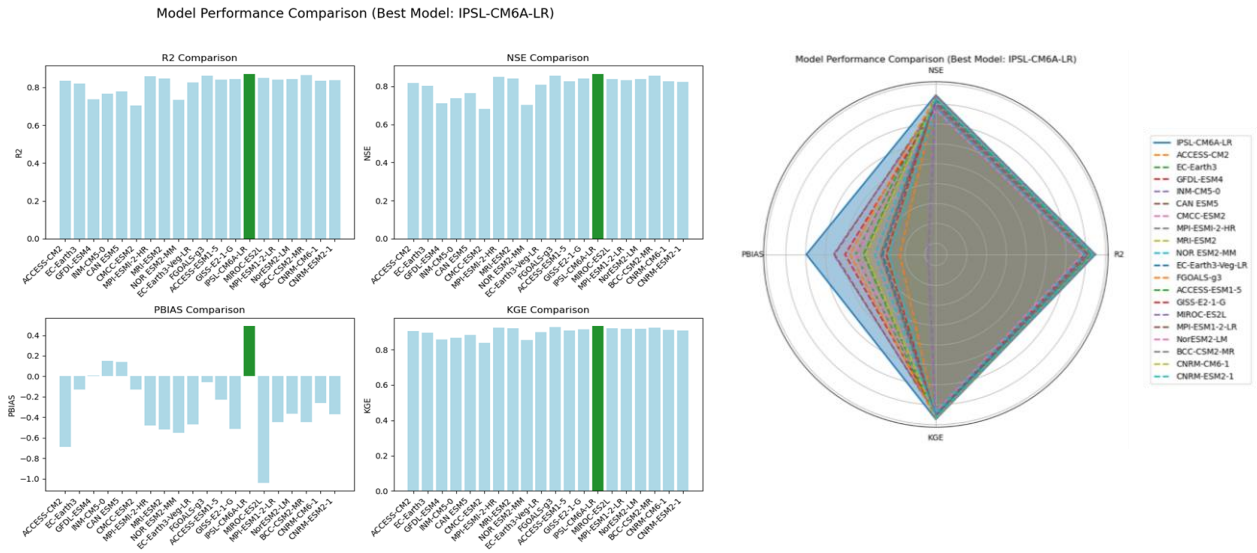

(a) Bar Chart (b) Radar Chart

Figure 3. Performance of various CMIP6 models to mimic TMAX over the study region in 1985-2014

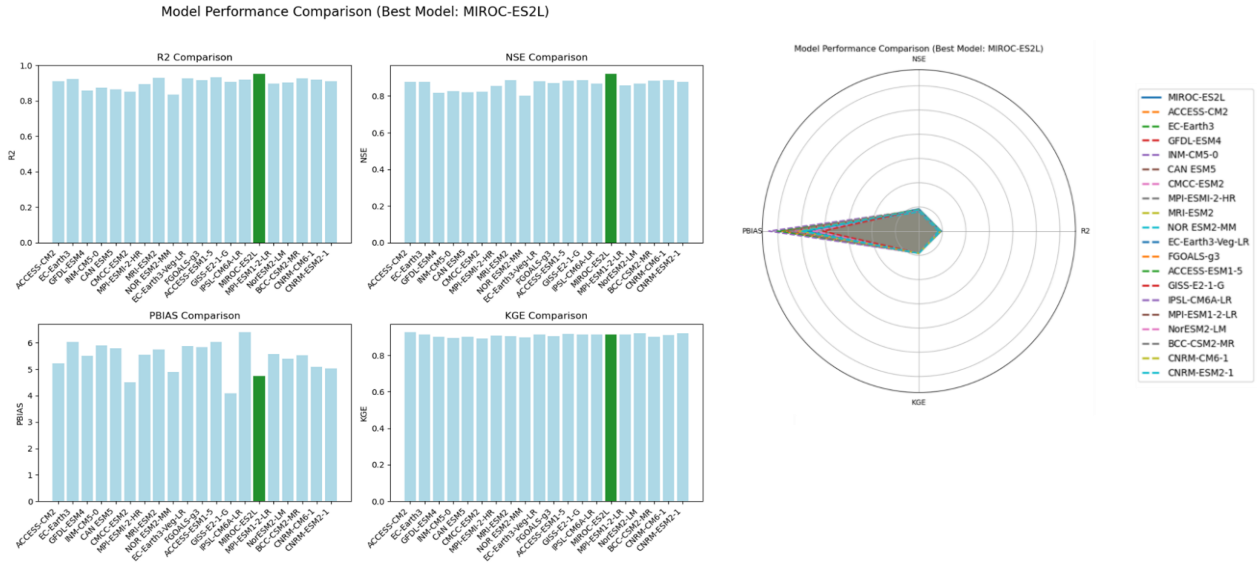

(a) Bar Chart (b) Radar Chart

Figure 4. Performance of various CMIP6 model to mimic TMIN over the study region in 1985-2014

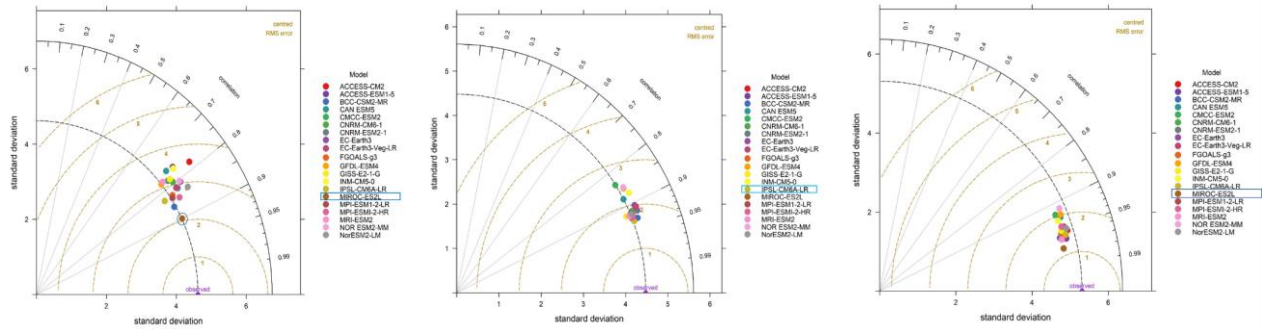

(a) Precipitation (b) TMAX (c) TMIN

Figure 5. Taylor diagram for different climatic variables obtained from various CMIP6 models versus observed IMD data over the study region in 1985-2014

similar to that of observational data. As a result, the overall performance of that model is superior to the other models for mimicking PPT over the study region. Similarly, IPSL-CM6A-LR outperforms the others when mimicking TMAX, and MIROC-ES2L performs better than the other models when mimicking TMIN, as illustrated in Figure 5.

Table 4 shows the basic statistical variation for the monthly mean of observed and the best CMIP6 model for PPT, TMAX, and TMIN during the years 1985 to 2014. It is found that the minimum, maximum, mean, and standard deviation for both datasets are nearly equivalent. The mean of monthly CMIP6 PPT data is 3.19 mm, which is approximately identical to the mean of observed PPT, which is 3.32 mm. While the standard deviation of CMIP6 monthly mean data is 4.62 mm, it is approximately comparable to the standard deviation of observed PPT, which is 4.63 mm. Similarly, the mean of CMIP6 TMAX monthly mean data is 31.96 ℃, which is approximately identical to the mean of observed TMAX, which is 32.23 ℃, and the standard deviation of CMIP6 TMAX monthly mean data is 4.53 ℃, which is nearly equivalent to the standard deviation of observed TMAX, which is 4.49 ℃. The mean of the CMIP6 TMIN monthly mean data is 27.94 ℃, which is quite similar to the mean of the observed TMIN, which is 27.12 ℃, and the standard deviation of CMIP6 TMIN is 4.94 ℃, which is nearly equivalent to the standard deviation of the observed TMIN, which is 5.31 ℃. This indicates that these models are most suited for replicating these climate variables. Since these models demonstrate superior performance compared to other models for historical periods, they can also be a preferred choice for projecting climate variables for future periods. This kind of investigation contributes in assessing the reliability of CMIP6 in mimicking climate variables. As a result, it was recognized that CMIP6 is a useful resource for decision-makers and researchers across numerous fields, supporting more well-informed strategies and actions in dealing with climate change challenges. Figure 6 shows the time series plots and scatter plots between IMD data and the best CMIP6 model data for the PPT, TMAX, and TMIN. This visual aid enables an in-depth examination of how well the model matches the real data for the historical period spanning from 1985 to 2014. This systematic representation makes it easier to comprehend the level of agreement between the values in the model and the observations, which offers important insights into the reliability as well as the effectiveness of the model. It is noteworthy that these models accurately capture the IMD data and may simulate the PPT, TMAX, and TMIN across the years. From the scatter plot, it is also evident that PPT is not as well simulated compared to TMAX and TMIN. This may be due to more complex patterns of PPT, which are impacted by a variety of factors so that the PPT can change dramatically over short distances and time periods, resulting in high spatial and temporal variability that climate models struggle to capture accurately.

5. Conclusions

To examine the changing climatic scenario, it is vital to use an appropriate climate model. CMIP6 provides an advanced framework for mimicking many components of the climate system of the earth, offering vital insights for sustainable water resource management and agricultural development. Precipitation, maximum and minimum temperatures are essential factors for assessing climate patterns since they have a large impact on atmospheric weather conditions. The primary objective of this study was to assess the performance of twenty coupled model intercomparison project phase 6 (CMIP6) global circulation models (GCMs) to mimic PPT, TMAX, and TMIN by comparing these models to observational data obtained from Indian Meteorological Department (IMD), Pune, for the Mahanadi River basin in Chhattisgarh from 1985 to 2014. The GCMs assessed in this study are derived from NASA's Earth Exchange Global Daily Downscaled Projections (NEX-GDDP). Several statistical metrics, such as the Coefficient of Determination (R^2), Nash-Sutcliffe efficiency (NSE), Kling-Gupta efficiency (KGE), Percent bias (PBIAS), and the Taylor diagram are utilized to assess the performance of these GCMS. The metrics are evaluated by comparing monthly mean simulated data from CMIP6 models and IMD observational data. The results obtained from this study suggest that the CMIP6 model MIROC-ES2L performs the best in mimicking PPT as compared to the other CMIP6 models, achieving in this study an R^2 of 0.81, an NSE of 0.80, and a KGE of 0.90 with respect to IMD observational PPT data. Similarly, in mimicking observed IMD TMAX, IPSL-CM6A-LR model outperforms the other models with an R^2 of 0.87, an NSE of 0.86, and a KGE of 0.93. The CMIP6 model, MIROC-ES2L surpasses the other CMIP6 models to replicate observed IMD TMIN data with an R^2 of 0.95, an NSE of 0.92, and a KGE of 0.91. Additionally, the calculated PBIAS values of all these best models obtained are under acceptable limits. Their mean and standard deviation are also almost equivalent to observational data. The graphical visualization of the performance using the Taylor diagram and Radar chart provides a clear visual understanding that aids in the identification of the most effective model and supports the outcomes from the quantitative statistical analysis.

Table 4. Comparison of the best CMIP6 model with IMD data

Variable	Model	Minimum	Maximum	Mean	Std. Deviation
PPT (mm)	IMD	0.00 mm	18.51 mm	3.32 mm	4.63 mm
	CMIP6 (MIROC-ES2L)	0.00 mm	16.90 mm	3.19 mm	4.62 mm
TMAX (℃)	IMD	23.58 ℃	42.28 ℃	32.23 ℃	4.49 ℃
	CMIP6 (IPSL-CM6A-LR)	23.33 ℃	43.36 ℃	31.96 ℃	4.53 ℃
TMIN (℃)	IMD	8.85 ℃	27.12 ℃	19.31 ℃	5.31 ℃
	CMIP6 (MIROC-ES2L)	10.25 ℃	27.94 ℃	20.16 ℃	4.94 ℃

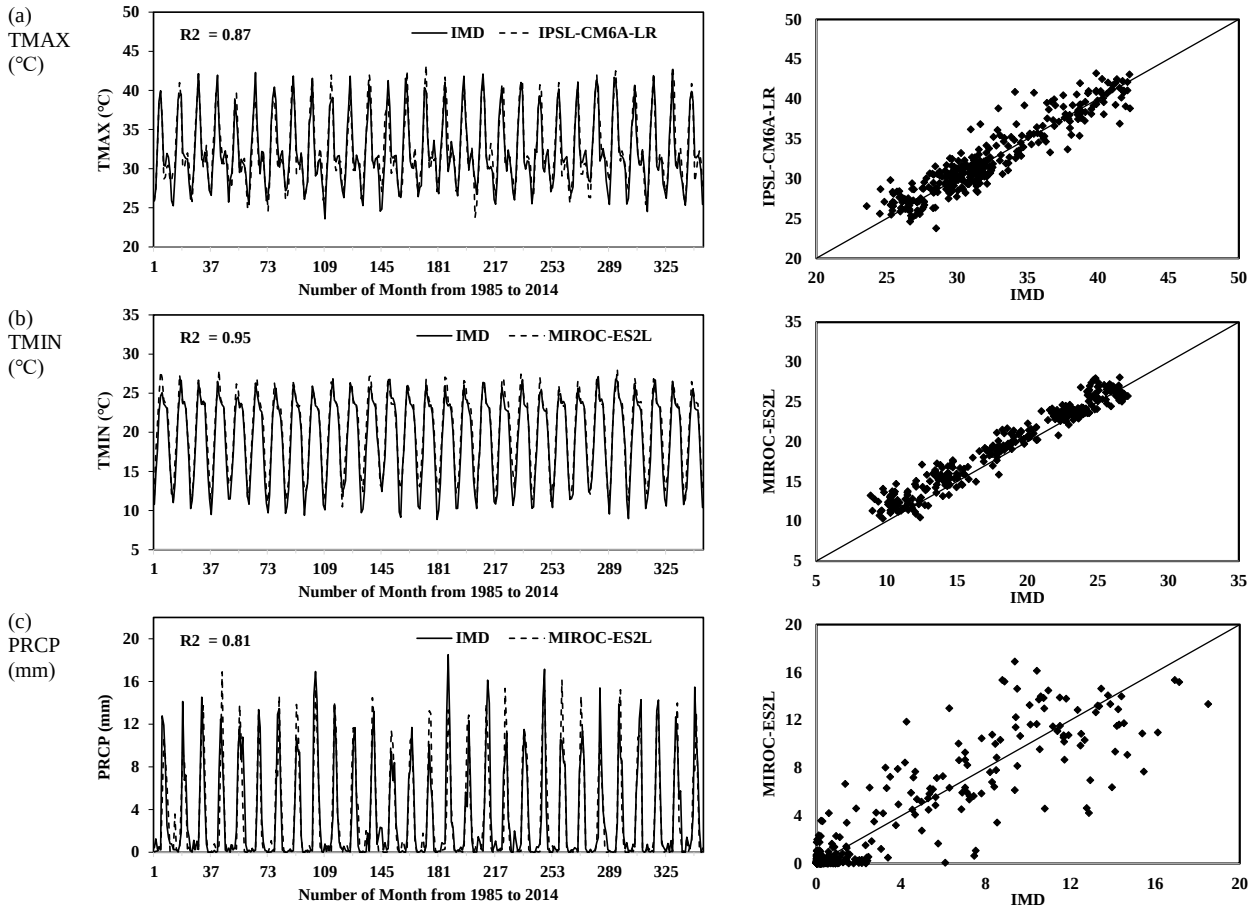

Figure 6. Time series and scatter plots between the best CMIP6 models and IMD data for different climatic variables in 1985 to 2014

It is hoped that the outcome of this study will help the researchers, hydrologists, and policymakers to select the most accurate climate models for mimicking different climatic variables for use in the monitoring and forecasting of various climatic factors at the local scale by utilizing standard statistical measures for the development of sustainable and adaptive water resource management strategies.

References

Ahmed, K., Sachindra, D. A., Shahid, S., Demirel, M. C., & Chung, E. S. (2019). Selection of multi-model ensemble of general circulation models for the simulation of precipitation and maximum and minimum temperature based on spatial assessment metrics. *Hydrology and Earth System Sciences*, *23*(11), 4803–4824. doi:10.5194/hess-23-4803-2019

Ali, Z., Iqbal, M., Khan, I. U., Masood, M. U., Umer, M., Lodhi, M. U. K., & Tariq, M. a. U. R. (2023). Hydrological response under CMIP6 climate projection in Astore River Basin, Pakistan. *Journal of Mountain Science*, *20*(8), 2263–2281. doi:10.1007/s11629-022-7872-x

Brunner, M. I., Slater, L., Tallaksen, L. M., & Clark, M. (2021). Challenges in modeling and predicting floods and droughts: A review. *Wiley Interdisciplinary Reviews Water*, *8*(3). doi:10.1002/wat2.1520

Chokkavarapu, N., & Mandla, V. R. (2019). Comparative study of GCMs, RCMs, downscaling and hydrological models: A review toward future climate change impact estimation. *SN Applied Sciences*, *1*(12). doi:10.1007/s42452-019-1764-x

Dibaba, W. T., Demissie, T. A., & Miegel, K. (2020). Watershed hydrological response to combined land use/land cover and climate change in highland Ethiopia: Finchaa catchment. *Water*, *12*(6), 1801. doi:10.3390/w12061801

Giorgi, F. (2019). Thirty years of regional climate modeling: Where are we and where are we going next? *Journal of Geophysical Research Atmospheres*, *124*(11), 5696–5723. doi:10.1029/2018jd030094

Gleckler, P. J., Taylor, K. E., & Doutriaux, C. (2008). Performance metrics for climate models. *Journal of Geophysical Research Atmospheres*, *113*(D6). doi:10.1029/2007jd008972

Gupta, H. V., Kling, H., Yilmaz, K. K., & Martinez, G. F. (2009). Decomposition of the mean squared error and NSE performance criteria: Implications for improving hydrological modelling. *Journal of Hydrology*, *377*(1–2), 80–91. doi:10.1016/j.jhydrol.2009.08.003

Haider, S., Masood, M. U., Rashid, M., Alshehri, F., Pande, C. B., Katipoğlu, O. M., & Costache, R. (2023). Simulation of the potential impacts of projected climate and land use change on runoff under CMIP6 scenarios. *Water*, *15*(19), 3421. doi:10.3390/w15193421

Hamed, M. M., Nashwan, M. S., & Shahid, S. (2022). A novel selection method of CMIP6 GCMs for robust climate projection. *International Journal of Climatology*, *42*(8), 4258–4272. doi:10.1002/joc.7461

Hazarika, N., Das, A. K., & Borah, S. B. (2015). Assessing land-use changes driven by river dynamics in chronically flood affected Upper Brahmaputra plains, India, using RS-GIS techniques. *The Egyptian Journal of Remote Sensing and Space Science*, *18*(1), 107–118. doi:10.1016/j.ejrs.2015.02.001

Hemanandhini, S. (2023). Performance evaluation of CMIP6 climate models for selecting a suitable GCM for future precipitation at different places of Tamil Nadu. *Environmental Monitoring and Assessment*, *195*(8). doi:10.1007/s10661-023-11454-9

Kushwaha, P., Pandey, V. K., Kumar, P., Sardana, D., & Yadav, A. (2024). Projection of mean and extreme precipitation and air temperature over India: a CMIP6 analysis. *Journal of Water and Climate Change*, 15(6), 2562–2581. doi.org/10.2166/wcc.2024.523

Lambert, S. J., & Boer, G. J. (2001). CMIP1 evaluation and intercomparison of coupled climate models. *Climate Dynamics*, *17*(2–3), 83–106. doi:10.1007/pl00013736

Legates, D. R., & McCabe, G. J. (1999). Evaluating the use of "goodness-of-fit" Measures in hydrologic and hydroclimatic model validation. *Water Resources Research*, *35*(1), 233–241. doi:10.1029/1998wr900018

Mathbout, S., Martin-Vide, J., & Bustins, J. A. L. (2023). Drought characteristics projections based on CMIP6 climate change scenarios in Syria. *Journal of Hydrology Regional Studies*, *50*, 101581. doi:10.1016/j.ejrh.2023.101581

Nash, J., & Sutcliffe, J. (1970). River flow forecasting through conceptual models part I — A discussion of principles. *Journal of Hydrology*, *10*(3), 282–290. doi:10.1016/0022-1694(70)90255-6

Ngai, S. T., Tangang, F., & Juneng, L. (2017). Bias correction of global and regional simulated daily precipitation and surface mean temperature over Southeast Asia using quantile mapping method. *Global and Planetary Change*, *149*, 79–90. doi:10.1016/j.gloplacha.2016.12.009

Raju, K. S., & Kumar, D. N. (2020). Review of approaches for selection and ensembling of GCMs. *Journal of Water and Climate Change*, *11*(3), 577–599. doi:10.2166/wcc.2020.128

Taylor, K. E. (2001). Summarizing multiple aspects of model performance in a single diagram. *Journal of Geophysical Research Atmospheres*, *106*(D7), 7183–7192. doi:10.1029/2000jd900719

Xie, H., Wei, G., Shen, Z., Dong, J., Peng, Y., & Chen, X. (2019). Event-based uncertainty assessment of sediment modeling in a data-scarce catchment. *CATENA*, *173*, 162–174. doi:10.1016/j.catena.2018.10.008

Zamani, Y., Monfared, S. a. H., Moghaddam, M. A., & Hamidianpour, M. (2020). A comparison of CMIP6 and CMIP5 projections for precipitation to observational data: the case of Northeastern Iran. *Theoretical and Applied Climatology*, *142*(3–4), 1613–1623. doi:10.1007/s00704-020-03406-x